The nondiffractive wave propagation in the sonic crystal consisting of rectangular rods with a slit

2008 J. Phys.: Condens. Matter 20 295229

(http://iopscience.iop.org/0953-8984/20/29/295229)

IOP Publishing Journal of Physics: Condensed Matter

J. Phys.: Condens. Matter **20** (2008) 295229 (6pp) doi:10.1088/0953-8984/20/29/295229

The nondiffractive wave propagation in the sonic crystal consisting of rectangular rods with a slit

Liang-Yu Wu, Lien-Wen Chen[1] and Mei-Ling Wu

Department of Mechanical Engineering, National Cheng Kung University, Tainan 70101, Taiwan

E-mail: chenlw@mail.ncku.edu.tw

Received 27 February 2008, in final form 4 June 2008
Published 1 July 2008
Online at stacks.iop.org/JPhysCM/20/295229

Abstract

This study investigates the nondiffractive propagation of sound waves in two-dimensional sonic crystals consisting of rectangular rods with a slit. The plane wave expansion method is used to calculate the equifrequency surfaces of sonic crystals with a square lattice. At certain frequencies, straight contour lines in the equifrequency surfaces are found. That frequency is strongly dependent on the geometric sizes of the rectangular rods. Further, the nondiffractive propagation of the sound wave can be realized for omnidirectional incident angles, and the properties can be applied to design novel acoustic devices.

(Some figures in this article are in colour only in the electronic version)

1. Introduction

During the past decade, the investigation of acoustic or elastic wave propagation in periodic composite materials, also called sonic crystals, has received increased attention. Such artificial crystals can exhibit acoustic or elastic band gaps in which sound and vibration are forbidden in any direction. This is of interest for applications such as elastic-acoustic waveguides, filters, and noise control. The band gaps are dependent on the filling fraction of the cylinders in the sonic crystal [1]. Further, a giant band gap had been found in the two-dimensional sonic crystal consisting of the air and water [2]. For the two-dimensional sonic crystal consisting of square rods, the acoustic band gaps can be controlled by rotating square rods [3]. The sonic crystal composed of hollow steel cylinders in a water background has been investigated [4]. Also, a narrow pass band is found in the band gaps, and the frequency of this narrow pass band can be tuned by varying the inner radius of the cylindrical tube inclusions. In addition, this study investigates the band structures of sonic crystals consisting of rods with various shapes and orientations [5]. The wave propagation in two-dimensional sonic crystals composed of a square array of hollow dielectric elastomer cylinders in an air background has also been studied [6]. The acoustic band gaps can be tuned by applying a voltage on the dielectric elastomer tubes.

Recently, the negative refraction behavior of photonic crystals has been discovered and has attracted much attention [7]. In addition to the negative refraction behavior, Kosaka *et al* has observed another outside-gap phenomenon showing collimated light propagation insensitive to the divergence of the incident beam [8]. This phenomenon is called self-collimation. Both of these, the negative refraction behaviors and the self-collimation phenomenon, can be analyzed by using the equifrequency surfaces (EFSs) of the photonic crystals. The integrated optics applications and devices with the self-collimation in the photonic crystal structures have been presented [9].

Analogous to the photonic crystals, the studies of acoustic and elastic wave propagation in sonic crystals have received increased attention. The negative refraction behavior of the sonic crystals has been discussed and the EFSs are used to predict the refraction direction [10, 11]. The dispersion characteristics of two-dimensional sonic crystals consisting of elliptic rods have also been reported [12]. By rotating the elliptic rods, different structure factors are obtained that vary the EFSs, and thus the refraction direction can then be tuned. In addition, the acoustic imaging and collimation by slabs of sonic crystals have been investigated [13]. In this

[1] Author to whom any correspondence should be addressed.

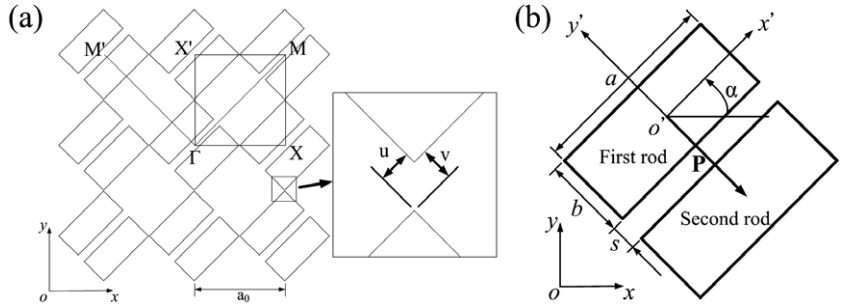

Figure 1. (a) The Brillouin zone of a square lattice sonic crystal consisting of square rods with a slit, where a_0 is the lattice constant. The inset shows that clearances exist between the unit cell and adjacent unit cell. (b) The unit cell considered in the plane wave expansion method is shown, where s is the width of the slit, α is orientation angle between the x and x' axes, and **P** denotes the position of the second rectangular rod in the unit cell from the first rod at the coordinate origin.

research, it is shown that within the partial band gaps, the acoustic waves tend to be collimated or guided into the direction in which the propagation is allowed. The pass band characteristics of wave propagation in two-dimensional thin plate sonic crystals have been analyzed by using the iso-frequency contour lines [14]. To clarify, the self-collimation is also called subdiffractive propagation or nondiffractive propagation, and is between the normal diffraction and negative diffraction propagation [15, 16]. This phenomenon has been predicted theoretically in sonic crystals [15] and demonstrated experimentally in a two-dimensional sonic crystal formed by a square array of steel cylinders immersed in water [16].

To obtain the band gaps and the refraction direction of a sonic crystal, a computation of the band structures and the EFSs is required. Several popular methods have been developed to calculate the band structures and the EFSs, i.e., (1) the plane wave expansion (PWE) method [2, 3], (2) the multiple-scattering theory (MST) method [17] and (3) the finite difference time domain (FDTD) method [18]. In addition, the finite element method (FEM) is also used to calculate band gaps and localized vibration modes for continuous and discrete periodic structures [19].

In this paper, the PWE method is employed to obtain the EFSs for finding the straight contour lines and the finite element commercial software, *COMSOL Multiphysics*® [20], is applied to simulate the pressure field in sonic crystals consisting of rectangular rods with a slit in an air background. Nondiffractive propagation for omnidirectional incident angles is found in the sonic crystal at the frequencies of the straight contours in the EFS. This research shows that the frequencies of the straight contour line depend strongly on the length, width of the rectangular rods and the width of the slit. The frequencies of the straight contour lines can be controlled by changing the parameters of the system. In addition, the properties of nondiffractive propagation for omnidirectional incident angles can be applied to design novel acoustic devices.

2. Numerical modeling

The two-dimensional periodic structure of the studied system is shown in figure 1. System is composed of rectangular rods with a slit in a fluid background. Since the fluid does not allow a transverse wave to propagate, only the longitudinal wave is only allowed. It is a good approximation to consider the solid rods as fluid inclusions with very high stiffness and specific mass. Then, the wave equation may be simplified as follows [2]:

$$(C_{11})^{-1}\frac{\partial^2 \boldsymbol{p}}{\partial t^2} = \nabla \cdot (\rho^{-1}\nabla \boldsymbol{p}) \tag{1}$$

where $\boldsymbol{p}$ is the pressure, ρ is the mass density, $C_{11} = \rho c_1^2$ is the longitudinal elastic constant and c_1 is the longitudinal speed of sound. The quantities $\rho^{-1}(\mathbf{r})$ and $C_{11}^{-1}(\mathbf{r})$ can be expanded by the Fourier series as given below [2]:

$$\rho^{-1}(\mathbf{r}) = \sum_G \sigma(\mathbf{G})\mathrm{e}^{\mathrm{i}\mathbf{G}\cdot\mathbf{r}}, \qquad \text{and} \qquad C_{11}^{-1}(\mathbf{r}) = \sum_G \zeta(\mathbf{G})\mathrm{e}^{\mathrm{i}\mathbf{G}\cdot\mathbf{r}} \tag{2}$$

where **G** are the 2D reciprocal lattice vectors. A periodic system of rods (medium A) in a background of medium B is proposed to be studied. The corresponding densities (elastic constants) are ρ_A, $\rho_B(C_{11A}, C_{11B})$. The rectangular rod with a slit can be taken as two rectangular rods. Then it is a simple matter to show that

$$\sigma(\mathbf{G}) = \begin{cases} 2\rho_A^{-1} f + \rho_B^{-1}(1-2f) \equiv \overline{\rho^{-1}}, & \text{for } \mathbf{G} = 0, \\ (\rho_A^{-1} - \rho_B^{-1})F(\mathbf{G}) \\ \quad + \mathrm{e}^{-\mathrm{i}\mathbf{G}\cdot\mathbf{P}}(\rho_A^{-1} - \rho_B^{-1})F(\mathbf{G}) \\ \quad \equiv \Delta(\rho^{-1})F(\mathbf{G}), & \text{for } \mathbf{G} \neq 0, \end{cases} \tag{3}$$

where f is the filling fraction of a rectangular rod and $F(\mathbf{G})$ is the structure factor. **P** denotes the position of the second rectangular rod in the unit cell from the first rod at the coordinate origin as shown in figure 1(b). An equation analogous to equation (3) can be written for $\zeta(\mathbf{G})$ in terms of C_{11}^{-1}. For a system of rectangular rods with orientation angle α between the x and x' axis, $F(\mathbf{G})$ can be written as:

$$F(\mathbf{G}) = f\frac{\sin(G'_x a/2)}{G'_x a/2}\frac{\sin(G'_y b/2)}{G'_y b/2}, \tag{4}$$

$$G'_x = G_x\cos\alpha + G_y\sin\alpha, \qquad G'_y = -G_x\sin\alpha + G_y\cos\alpha, \tag{5}$$

where a is the length and b is the width of rectangular cross section of rods. For square lattices with lattice constant of a_0, the filling fraction f is given by

$$f = \frac{ab}{a_0^2}. \tag{6}$$

With the aid of the Bloch theorem, equations (2), and (3), the eigenvalue equation is obtained as follows [2]:

$$\sum_{\mathbf{G}'\neq\mathbf{G}} F(\mathbf{G}-\mathbf{G}')[\Delta(\rho^{-1})(\mathbf{K}+\mathbf{G})\cdot(\mathbf{K}+\mathbf{G}') - \Delta(C_{11}^{-1})\omega^2]\boldsymbol{p}_{\mathbf{K}}(\mathbf{G}') + [\overline{\rho^{-1}}|\mathbf{K}+\mathbf{G}|^2 - \overline{C_{11}^{-1}}\omega^2]\boldsymbol{p}_{\mathbf{K}}(\mathbf{G}') = 0. \tag{7}$$

where $\mathbf{K}$ is a 2D Bloch vector, $\omega(\mathbf{K})$ and $\boldsymbol{p}_{\mathbf{K}}(\mathbf{G})$ are the eigenvalues and eigenvectors, respectively.

The reciprocal lattice vectors are $\mathbf{G} = (2\pi/a_0)(n\vec{b}_1 + m\vec{b}_2)$, where $\vec{b}_1 = (1, 0)$, $\vec{b}_2 = (0, 1)$ for square lattices with a lattice constant a_0, and m, n are integers. In the PWE calculations, a total of 625 plane waves ($-12 \leqslant m, n \leqslant 12$) have been used. The band structure and EFS can be obtained by solving the eigenvalue equation (7).

The *COMSOL Multiphysics*® software is adopted to simulate the acoustic wave propagation in the sonic crystals [20]. The equation used to analyze the acoustic wave problems is expressed as,

$$-\nabla\cdot\frac{\nabla\boldsymbol{p}}{\rho} = \frac{\omega^2}{\rho c_1^2}\boldsymbol{p}. \tag{8}$$

By solving equation (8), the pressure field can be obtained in the sonic crystal.

3. Results and discussion

A two-dimensional sonic crystals consisting of the square steel rods with a slit in the air background is studied, where $\rho_{\text{steel}} = 7800\ \text{kg m}^{-3}$, $\rho_{\text{air}} = 1.2\ \text{g m}^{-3}$, $c_{\text{steel}} = 6100\ \text{m s}^{-1}$, $c_{\text{air}} = 343\ \text{m s}^{-1}$ (sound velocity in air at 20 °C). The lattice constant a_0 of the sonic crystal is 10 mm, the length of the rectangular rod is $a = 7$ mm, the width of the rectangular rod is $b = 2$ mm, and the width of the slit is $s = 3$ mm. The two rectangular rods and a slit form a 7 mm × 7 mm square rod. Figure 2(b) shows its band structure, and the band structure of the square rods (7 mm × 7 mm) without a slit is shown in the figure 2(a). It can be observed that a band gap exists between the first and second band in figure 2(a). A special band is found in that band gap when the square rods of the sonic crystal have a slit. That is the second band in figure 2(b). The EFS of the second band is adopted to investigate the wave propagation in the sonic crystal.

The EFS computed by the PWE method is used to predict the refraction direction. The direction of group velocity, i.e., the refraction direction, is determined by the gradient of the frequency in k-space, $V_{\text{g}} = \nabla_k\omega(k)$. The refraction direction can be obtained by analyzing the EFS [10–12]. The EFS of the second band is shown in figure 3. The case of $\alpha = 0°$ is plotted in figure 3(a). As can be observed, the EFS contours are all curves; no straight line exists. In figure 3(b), the

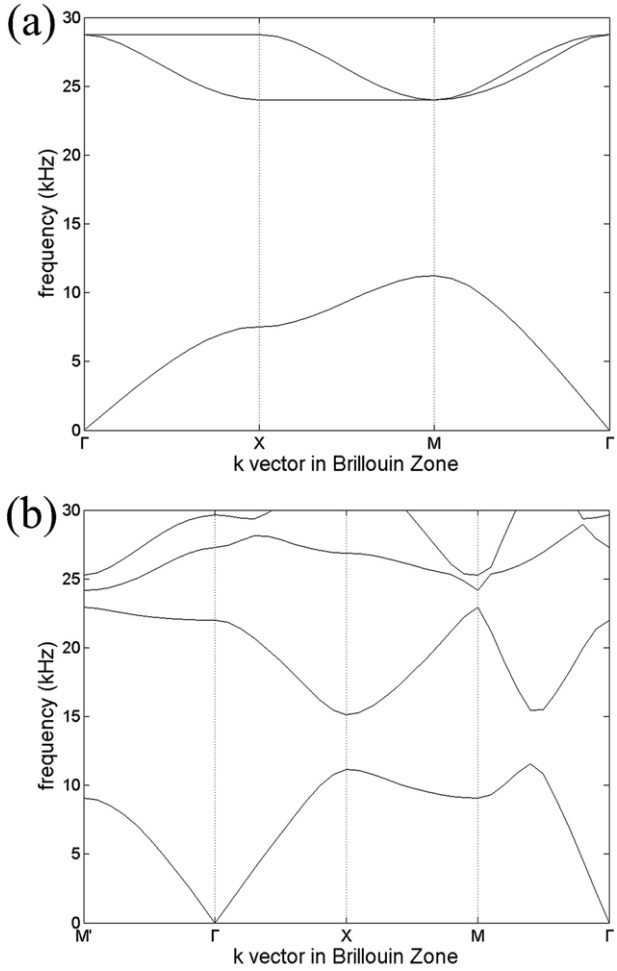

Figure 2. (a) The band structure of the square rods (7 mm × 7 mm) without a slit. (b) The band structure of the square rods with a slit ($a = 7$ mm, $b = 2$ mm, and $s = 3$ mm).

orientation angle α is 45°, and the contours of the frequencies are approximately straight lines, especially at 21.5 kHz. The frequency of the straight contour line becomes 22.49 kHz when the width of the slit is 0.5 mm as shown in figure 3(c). That is, the frequencies of the straight contour lines are dependent on the geometric size of the rods in the sonic crystals. The acoustic wave propagation in a sonic crystal is governed by its dispersion surface. The wave is only allowed to propagate along directions normal to the dispersion surface. Therefore, the refraction direction is perpendicular to the straight contour line of the EFSs. Figure 3(d) shows that the refraction directions are all the same at 21.5 kHz. The dash–dot circle and the solid lines stand for the EFS of air and the sonic crystal, respectively. The arrow K_{air} in the dash–dot circle represents the propagation direction of the incident wave, and is regarded as the wavevector of air. The arrow V_{g}, the group velocity, is the refraction direction of the acoustic wave in sonic crystals. As the sonic crystal is arranged along the Γ–M direction, nondiffractive propagation of the sound wave can be realized for all incident angles and the refraction angles are always zero.

Note that the certain frequency contour lines of the EFSs are square for the sonic crystal consisting of the circle steel

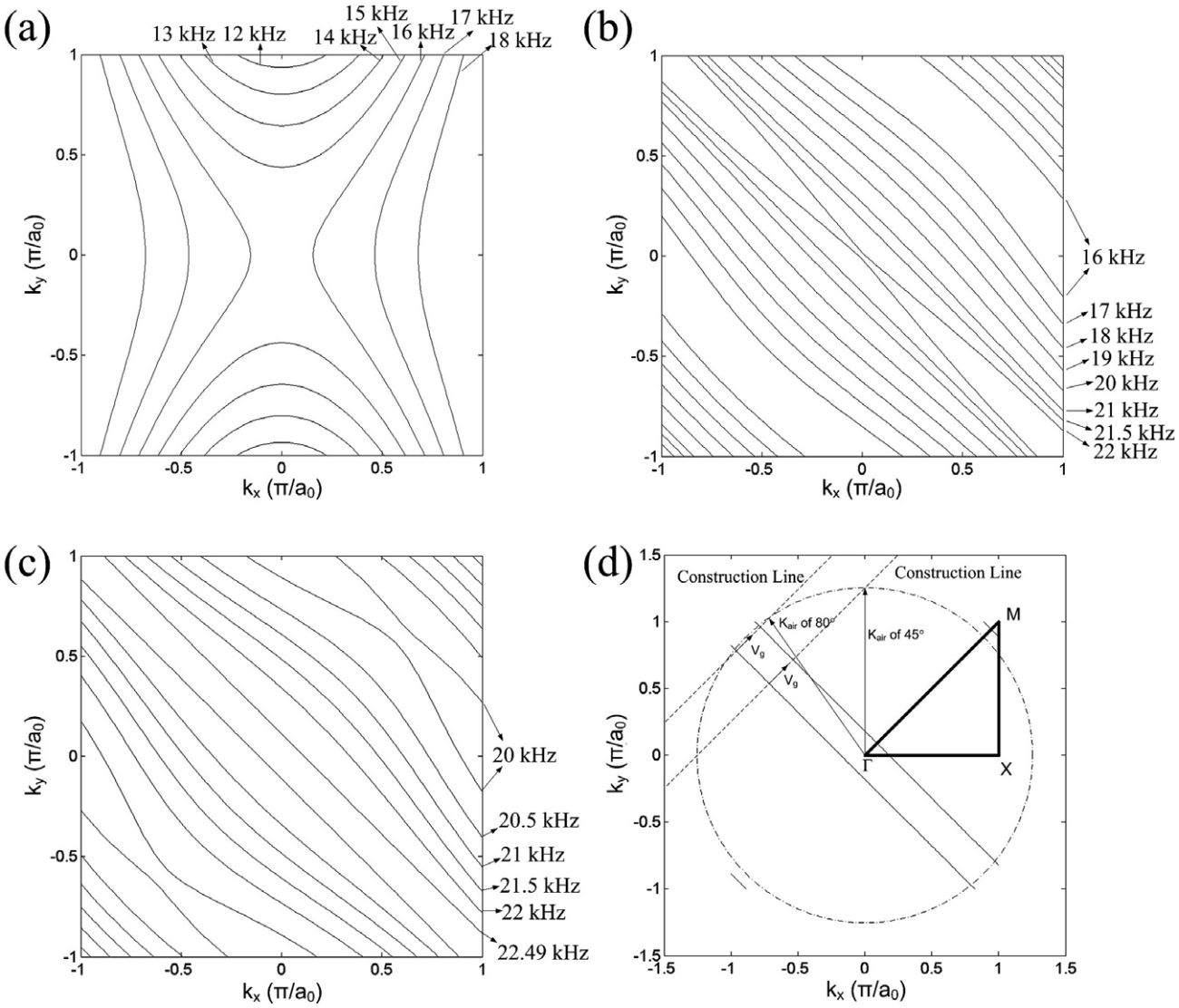

Figure 3. The EFSs of the second band for (a) $\alpha = 0°$ and (b) $\alpha = 45°$ are shown, where $a = 7$, $b = 2$, and $s = 3$ mm. (a) shows that all contour line are curve lines. In (b), the 21.5 kHz contour line is approximately a straight line. (c) shows the EFSs of the second band for $\alpha = 45°$, $a = 7$ mm, $b = 3.25$ mm, and $s = 0.5$ mm. The 22.49 kHz contour line is approximately a straight line. (d) shows that the refraction directions are the same at 21.5 kHz. The arrow V_g is the refraction direction of the acoustic wave in sonic crystals.

rods in a fluid background. The phenomena of nondiffractive propagation appear only in a small range of incident angles on the flat segments [15, 16]. However, there exist negative refractions and partial band gaps for large incident angles. In the present investigation, the analysis of the EFSs shows that the refraction direction is independent of the incident angles at the frequency of the straight contour line. Nondiffractive propagation and a 0° refraction angle are observed for omnidirectional incident angles in the sonic crystal arranged along the Γ–M direction. This phenomenon is sensitive to the frequency of the incident wave. It can be seen that the straight EFS contours occur only at the frequency of 21.5 kHz in figure 3(b). The contours of the other frequencies are all curved lines and not straight enough to achieve nondiffractive propagation for omnidirectional incident angles.

Figure 4 shows that the frequencies of the straight contour lines are a function of the length of the rectangular rods a for different width of the slits s at $2b + s = 7$ mm. It is revealed that the frequencies of the straight contour lines decrease linearly as the length of a increases. On the other hand, figure 5 shows that the frequencies of the straight contour lines are a function of the length of $2b + s$ for different width of the slits s at $a = 7$ mm. The frequencies of straight contour lines increase linearly as the length of $2b + s$ increases. The frequencies are proportional to the length of a and $2b + s$. The variations of the frequencies with a are greater than with $2b+s$. It is worth noticing that the straight contour lines of the EFSs cannot be found for smaller lengths of a and $2b + s$. For example, at $s = 0.5$ mm and $2b+s = 7$ mm, a straight contour line of the EFS cannot be found if the length of the rectangular rods $a < 6.85$ mm.

Moreover, we can observe the straight contour lines of the EFSs in the cases at $a = 7$ mm and $2b + s > 7$ mm. Figure 6 shows that the frequency of the straight contour lines of the

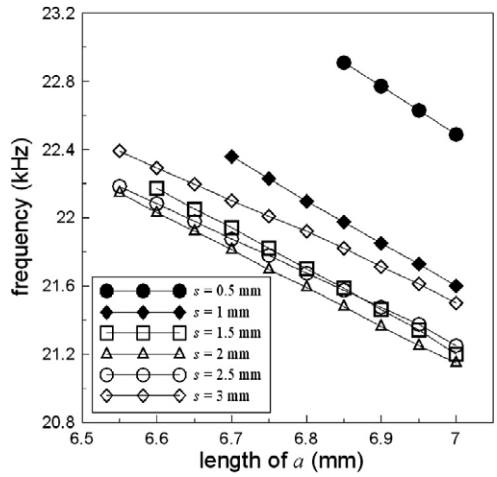

Figure 4. The frequencies of straight contour lines are a function of the length of the rectangular rods, a, and the width of the slits, s, at $2b + s = 7$ mm.

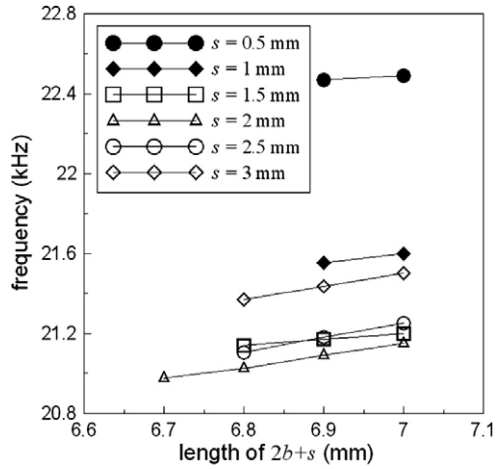

Figure 5. The frequencies of straight contour lines are a function of the length $2b + s$ and the width of the slits, s, at $a = 7$ mm.

EFS are a function of the width of a slit for different lengths of $2b + s$ at $a = 7$ mm. One can easily find that the frequency of straight contour lines decreases gradually with an increase of the width of a slit at a certain value of $2b + s$ until a critical value and then increases. For the same width of a slit, the larger the length $2b+s$, the higher is the frequency of straight contour lines. The phenomena of the straight contour lines was studied until the width of the rectangular rods b reduced to 2 mm. Note that, for $2b+s = 9$ mm, a straight contour line cannot be found if $s > 3$ mm i.e. $b < 3$ mm. The parameters of a, $2b+s$, and s can be controlled to tune the frequency of the straight contour line.

The FEM is also used to simulate wave propagations in the sonic crystal. A square lattice slab with eight layers is investigated. The sonic crystal ($a_0 = 10$ mm, $a = 7$ mm, $b = 2$ mm, and $s = 3$ mm) of a slab arranged in the Γ–M direction with 8 layers is used in this study. It is noted that the frequency of the acoustic wave is taken to be 21.5 kHz for all simulations in the this report. The

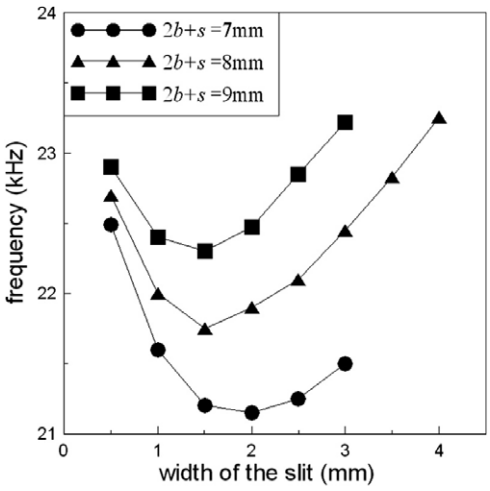

Figure 6. The frequencies for the straight contour lines of the EFSs are a function of the width of the silt, s, and the width of $2b + s$ at $a = 7$ mm.

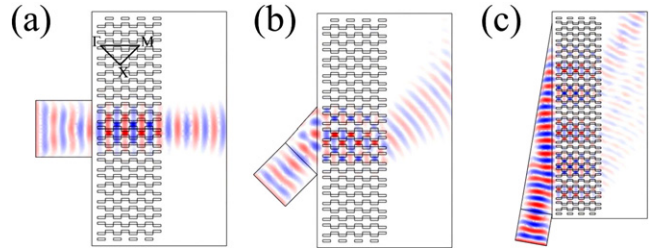

Figure 7. The pressure fields of simulation at different incident angle (a) 0°, (b) 45° and (c) 80° are displayed, respectively. All the acoustic waves propagate in the 0° refraction direction in the sonic crystal.

pressure field of the acoustic wave propagated through the crystal is shown in figure 7. We can see that there is obvious refraction behavior for the waves of 45° and 80° incident angles. All the acoustic waves propagate in the 0° refraction direction in the sonic crystal, and the direction of the transmitted waves is parallel to the incident wave. The refraction angle at 21.5 kHz is zero for omnidirectional incident angles. It also confirms that the direction of refraction is the same as that previously predicted by the EFS in figure 3(d). This sonic crystal is useful as a waveguide for omnidirectional incident directions in the absence of defects. Figure 8 shows a simulation of the acoustic wave propagation without and with the sonic crystal. It can be seen that the acoustic waves at 21.5 kHz radiate from the source in the homogeneous media in figure 8(a), and the width of the wave beam broadens appreciably over the propagation distance. The frequency of incident waves is 21.5 kHz and 18 kHz in figures 8(b) and (c), respectively. The acoustic wave beam propagates through the crystal without a visible divergence, as shown in figure 8(b). In figure 8(c), the wave beam propagates in the sonic crystal, which is the same as figure 8(b), and the wave beam broadens slightly over the propagation distance. The effect of nondiffractive propagation at 21.5 kHz is convincing. Moreover, the frequencies of the nondiffractive propagation and the waveguide can be

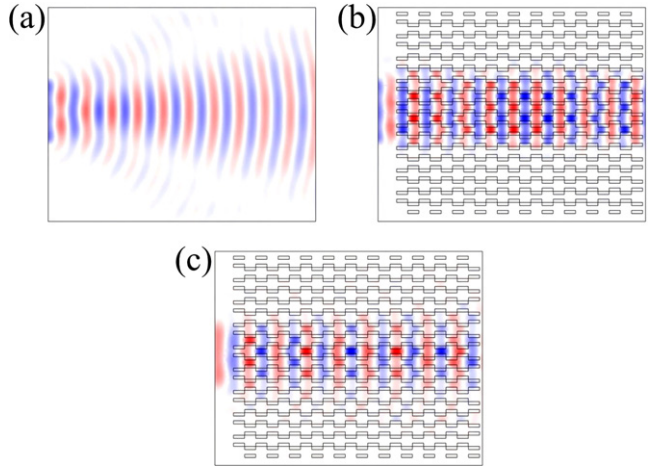

Figure 8. (a) The acoustic waves propagating in a homogeneous medium without the sonic crystal. (b) The acoustic waves at 21.5 kHz propagate in the sonic crystal. The acoustic wave beam propagates without a visible divergence. (c) The acoustic waves at 18 kHz propagate in the sonic crystal. The width of the wave beam broadens slightly over the propagation distance.

controlled by adjusting the size of the rectangular rods of the sonic crystal.

4. Conclusion

The nondiffractive propagation of the sound wave was studied in the two-dimensional sonic crystal. The sonic crystals are composed of rectangular rods with a slit. The EFSs of this sonic crystal have straight contour lines for certain frequencies. The refracted acoustic waves can propagate with 0° refraction angle for all incident angles in the proposed sonic crystals. The frequency of the straight contour line is dependent on the size of the rectangular rods and slits. By varying the size of the rectangular rods such as the length, width of rectangular rods, and the width of a slit, the frequency of the straight contour line can be selected. Tunable sonic crystals composed of a functional material will be the focus of our future studies. There the frequencies of the straight contour line can be controlled by applying an electric voltage.

Acknowledgment

The authors sincerely acknowledge the financial assistance of the National Science Council of Taiwan under the grant no. NSC 95-2221-E-006-040-MY2.

References

[1] Kushwaha M S 1997 *Appl. Phys. Lett.* **70** 3218
[2] Kushwaha M S and Djafrari-Rouhani B 1998 *J. Appl. Phys.* **84** 4677
[3] Wu F, Liu Z and Liu Y 2002 *Phys. Rev.* E **66** 046628
[4] Khelif A, Deymier P A, Djafari-Rouhani B, Vasseur J O and Dobrzynski L 2003 *J. Appl. Phys.* **94** 1308
[5] Zhong L, Wu F, Zhang X, Zhong H and Zhong S 2005 *Phys. Lett.* A **339** 164
[6] Yang W P and Chen L W 2008 *Smart Mater. Struct.* **17** 015011
[7] Notomi M 2000 *Phys. Rev.* B **62** 10696
[8] Kosaka H, Kawashima T, Tomita A, Notomi M, Tamamura T, Sato T and Kawakami S 1999 *Appl. Phys. Lett.* **74** 1212
[9] Prather D W, Shi S, Murakowski J, Schneider G J, Sharkawy A, Chen C, Miao B L and Martin R 2007 *J. Phys. D: Appl. Phys.* **40** 2635
[10] Zhang X and Liu Z 2004 *Appl. Phys. Lett.* **85** 341
[11] Feng L, Liu X P, Lu M H, Chen Y B, Y Chen F, Mao Y W, Zi J, Zhu Y Y, Zhu S N and Ming N B 2006 *Phys. Rev.* B **73** 193101
[12] Wu L Y and Chen L W 2007 *J. Phys. D: Appl. Phys.* **40** 7579
[13] Chen L S, Kuo C H and Ye Z 2004 *Appl. Phys. Lett.* **85** 1072
[14] Wen J, Yu D, Wang G, Zhao H, Liu Y and Wen X 2007 *Phys. Lett.* A **364** 323
[15] Pérez-Arjona I, Sánchez-Morcillo V J, Redondo J, Espinosa V and Staliunas K 2007 *Phys. Rev.* B **75** 014304
[16] Espinosa V, Sánchez-Morcillo V J, Staliunas K, Pérez-Arjona I and Redondo J 2007 *Phys. Rev.* B **76** 140302(R)
[17] Kafesaki M and Economou E N 1999 *Phys. Rev.* B **60** 11993
[18] Cao Y, Hou Z and Liu Y 2004 *Solid State Commun.* **132** 539
[19] Movchan A B, Movchan N V and Haq S 2006 *Mater. Sci. Eng.* A **431** 175
[20] *COMSOL 3.4a* The COMSOL Group. Stockholm, Sweden